TRANSCONDUCTOR AND INTEGRATOR CIRCUITS FOR INTEGRATED BIPOLAR VIDEO FREQUENCY FILTERS

W.J.A. de Heij E. Seevinck* K. Hoen

University of Twente, P.O. Box 217, Enschede, the Netherlands.
*Also with Philips Res. Labs., P.O. Box 80000, Eindhoven, the Netherlands.

Abstract

This paper describes novel transconductor and an integrator circuits which can be used in integrated video frequency filters in bipolar technology. The transconductor consists of a parallel connection of a passive nominal transconductance and an active variable transconductance, resulting in good high frequency performance up to 70 MHz and less than 1% linearity error for input signals up to $2V_{pp}$. In the integrator an operational transconductance amplifier circuit is used which provides tunable integrator phase. Simulation results of all circuits and of a fifth order elliptic lowpass filter with a nominal cutoff frequency of 5 MHz are presented.

Introduction

Bipolar technology has been used recently to realize continuous-time filters at video frequencies operating from a single 5 V supply [1],[2]. Modern combined bipolar-CMOS processing allows the combination of analog bipolar filters with CMOS digital logic on one chip, thus extending the range of application of bipolar filters.

Until now most integrated filters at video frequencies are of the transconductor-C class [1], [3]-[5]. In this class of filters it is difficult to design bipolar circuits having the same signal handling capability as the CMOS circuits. Linearization techniques such as emitter degeneration force the designer to trade off linearity against tunability [1] unless voltage tuned junction capacitors are used [5]. The high transconductance of the bipolar transistor can not be fully used in transconductor-C filters due to its exponential dependence on the base-emitter voltage.

In active-RC filters however the high transconductance of the bipolar transistor can be used effectively in the design of amplifiers with high GB-product and low output resistance. In this paper novel transconductor and amplifier circuits are presented which extend the operating range of active-RC filters beyond video frequencies. The transconductor circuit combines both good linearity and tunability. The circuits are balanced, resulting in better PSRR, less crosstalk through the substrate, and cancellation of some parasitic effects and nonlinearities.

The authors wish to thank B. Nauta and R.F. Wassenaar for their comments and fruitful discussions.

Tunable transconductor design

In a balanced active-RC integrator the input branch consists of two matched resistors with a nominal value R_1 following from filter synthesis. If oxide capacitors are used the resistors have to be made variable to tune the filter poles and zeros to their correct positions against production spread (±20% for a modern process) and temperature variations. A tunable trans- conductor can be realized by connecting a variable transconductance G_T, realized by an active circuit and having positive or negative values (nominally zero) in parallel with the resistors R_1 as shown in fig. 1.

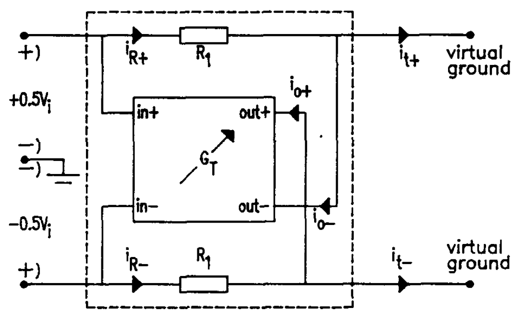

Fig. 1: Tunable transconductor principle.

The variable transconductance is defined by:

$$G_T = \frac{i_{o+} - i_{o-}}{v_i} \qquad (1)$$

For the complete transconductor we find:

$$G = \frac{i_{t+} - i_{t-}}{v_i} = \frac{1}{R_1} + G_T \qquad (2)$$

So we have created a tunable transconductance G which is varied around a nominal design value $1/R_1$ since the nominal value of G_T is zero. The parallel connection shown in fig. 1 has significant advantages in integrated filter applications where a deviation from the unity gain frequency $\omega_0 = 1/R_1C$ has to be corrected by tuning. In a well controlled process $|G_T| < 0.2/R_1$ is a realistic value [6]. Therefore G_T will be small, resulting in the following advantages:

CH2692-2/89/0000-0114 $1.00 © 1989 IEEE

1) The high frequency performance is dominated by the resistors R_1, instead of the active circuit, resulting in a very small phase shift at video frequencies.

2) The negative effect of non-linearity of the active circuit on the linearity of the complete transconductor is relatively small.

3) The active circuit can operate at low bias currents thus adding little noise to the thermal noise of the resistors R_1.

The influence of non-idealities of the active circuit is limited by the amount of tuning needed in the integrated filter. Fig. 2 shows a circuit realization of the transconductor principle. The variable transconductance G_T consists of the resistors R_2 and the npn-transistors Q_1 to Q_6. Using the translinear principle and eq. 2 we can find for the transconductance G:

$$G = \frac{i_{t+} - i_{t-}}{v_i} = \frac{1}{R_1} + \frac{I_1 - I_2}{I_3} * \frac{1}{R_2} \qquad (3)$$

The maximum differential input signal amplitude is mainly determined by I_3 and R_2:

$$V_{imax} \approx 2 I_3 R_2 \qquad (4)$$

For a given value of I_3 the amount of tuning depends on I_1-I_2 and R_2. For small values of I_1-I_2 most of the noise produced by Q_5, Q_6 and the resistors R_2 is eliminated within the circuit by the cross-coupled pairs Q_1,Q_2 and Q_3,Q_4. In that case Q_1-Q_4 produce most of the output noise. Therefore the sum current I_1+I_2 should not be made larger than is necessary for the expected values of I_1-I_2 needed for tuning.

The circuit has good high-frequency performance. The feed-forward currents through the base-collector capacitances of Q_1 to Q_4 cancel each other if balanced signals are applied to the circuit. It is possible to obtain a flat phase characteristic almost independent of tuning by including capacitors C_1 and C_2. C_1 compensates for the phase of R_1, while C_2 compensates for the phase of R_2 and the active circuit.

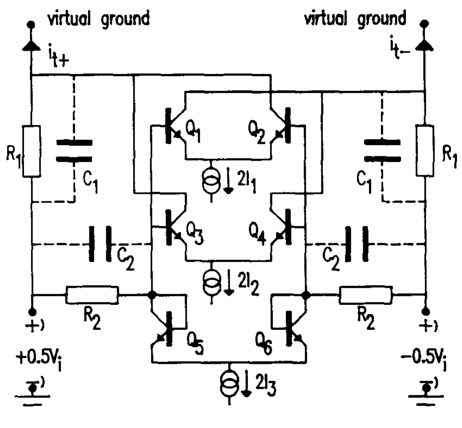

Fig. 2: Circuit realization of complete transconductor.

Fig. 3 shows a simulation of the transconductance G as a function of the input voltage. We have chosen $R_1=6k\Omega$, $R_2=4k\Omega$, $I_3=150\mu A$, and $I_1+I_2=50\mu A$. Results are shown for +20%, +10%, 0%, -10% and -20% tuning with respect to $1/R_1$.

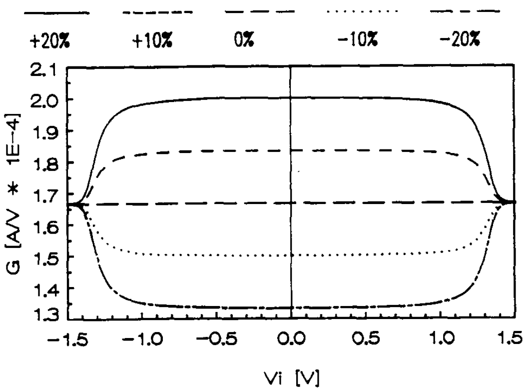

Fig. 3: Transconductance G versus input voltage.

The input voltages where 1% deviation from the transconductance at $V_i=0$ is found are 1.02V, 1.13V, 1.10V and 0.95V for +20%, +10%, -10% and -20% tuning. In case of +10% tuning the 1% error is caused by a 10.7% error of the variable transconductance G_T, which shows the reduced effect of nonlinearity of the active circuit.

In fig. 4 phase characteristics are shown for the same parameters used in fig. 3 and $C_1=14.3fF$ and $C_2=48fF$, using a frequency dependent model for base diffused resistors [7]. The phase characteristics stay very close to 0° for video frequencies. In practice there will be small deviations due to process tolerances. In high-Q applications they can be corrected by phase tuning, which will discussed in the next section.

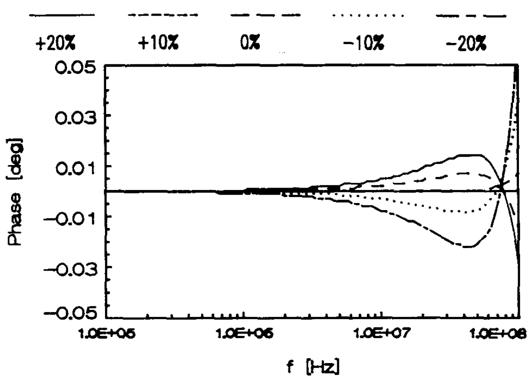

Fig. 4: Phase characteristics for different tuning.

It can be concluded that the transconductor principle results in good performance with respect to both linearity and high frequency performance. Its performance has an optimum for the nominal case ($G_T=0$).

The active-RC integrator

Fig. 5 shows the concept for the tunable active-RC integrator. The transconductor described in the previous section is used to tune the unity gain frequency ω_0, while variable resistors R_Q in the feedback path are used to tune the phase of the integrator. Instead of an operational voltage amplifier a transconductance amplifier (OTA) having transconductance G_A is used. If the OTA is assumed to have input resistance r_i and output resistance r_o the following transfer function is found:

$$\frac{v_o}{v_i} = \frac{r_i(1+R_1G_T)}{R_1+r_i} * \frac{-G_A r_o\left\{1 - sC\left\{\frac{1}{G_A} - R_Q\right\}\right\}}{1 + sC\left\{r_o + R_Q + (1+G_A r_o) * \frac{R_1 r_i}{R_1+r_i}\right\}} \qquad (5)$$

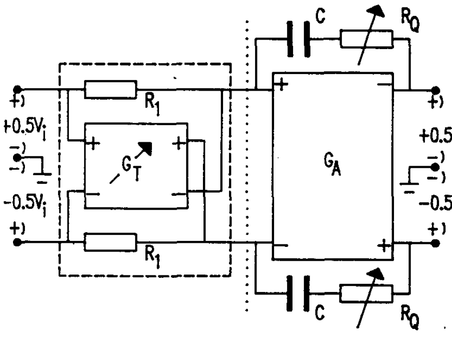

Fig. 5: Active-RC integrator concept.

From eq. 5 we find the following parameters of the integrator:

$$\text{D.C.-gain:} \quad |A_{DC}| = \frac{r_i}{R_1+r_i}(1+R_1G_T)\, G_A r_o \qquad (6)$$

$$\text{Unity gain frequency:} \quad \omega_o \approx \frac{G_A(1+G_TR_1)}{(1+G_AR_1)C} \approx \frac{1+G_TR_1}{R_1C} \qquad (7)$$

Eqs. 6 and 7 show that ω_o and A_{DC} are both equally tuned by the variable transconductance G_T. A more detailed analysis shows that this is caused by the current source output of the variable transconductance G_T. At DC the output current of G_T is forced through the resistors R_1 and the input resistance r_i of the OTA resulting in an additional voltage gain of $1+R_1G_T$ in the transfer function from the integrator input voltage V_i to the input voltage of the OTA. For sufficient nominal DC-gain and $|R_1G_T|<0.2$ this has little effect.

Eq. 5 also indicates that the integrator has a high frequency zero. For $R_Q=0$ the zero is located in the right-half-plane. If $R_Q=1/G_A$ the zero is placed at infinity. If $R_Q>1/G_A$ the zero is moved into the left-half plane where it can be used to compensate for the excess phase caused by parasitic poles and zeros of the circuit. For high-Q applications R_Q can be made variable so that the phase of the integrator can be tuned. Automatic phase tuning circuits have already been reported in literature on high frequency integrated filters [4],[8].

The OTA circuit

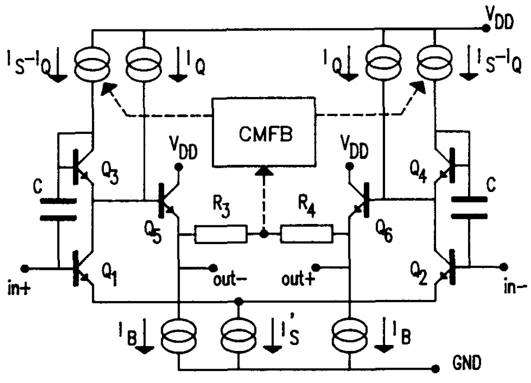

Fig. 6: OTA with feedback path and output buffers.

Fig. 6 shows the OTA with the feedback path to the right of the dotted line in fig. 5. The OTA consists of Q_1 and Q_2, biased by $I_s'\approx 2I_s$. Q_3 and Q_4 act as the variable resistors R_Q. If $I_Q=0$ the collector current of Q_3 and Q_4 is given by:

$$I_{c3} \approx I_{c1} \qquad I_{c4} \approx I_{c2} \qquad (8)$$

Then $R_Q\approx 1/G_A$ where G_A is the transconductance of Q_1 and Q_2 and the zero is placed at infinity. If $I_Q>0$ I_{c3} and I_{c4} become smaller than I_{c1} and I_{c2} resulting in $R_Q>1/G_A$ and the zero is placed in the left-half-plane. The use of diodes Q_3 and Q_4 has two more important advantages besides tunability:

1) If I_Q is not too large compared to I_S the diodes also provide large signal tracking of R_Q with $1/G_A$ and the variation of the base-emitter voltage U_{be3} (U_{be4}) compensates the variation of U_{be1} (U_{be2}) thus reducing harmonic distortion.

2) At high frequencies the impedance of the diodes has a zero at almost the same position as the zero in $1/G_A$ (both caused by the base resistance) extending the frequency range where the compensation is effective.

The current I_s-I_Q through Q_3 and Q_4 is established by a common-mode feedback circuit, which senses the common mode output voltage with a resistive divider with $R_3=R_4$ driven by Q_5 and Q_6. At DC the output impedance at the emitters of Q_3 and Q_4 is high so that output buffers Q_5 and Q_6 (not shown in fig. 5) are necessary to maintain sufficient DC-gain since the outputs are loaded by transconductors shown in fig. 2. The total bias current of these transconductors flows also through Q_5 and Q_6, adding up to the bias current I_B in fig. 6.

Fig. 7 shows integrator simulations for -20%, 0% and +20% tuning of the unity gain frequency. For the OTA $I_s'=I_B=500\mu A$. $R_1=6k\Omega$ and $C=5.0pF$. In case of 0% tuning a unity gain frequency ω_0 of 5.0MHz is found, which is 0.1MHz lower than the value found from eq. 5 or eq. 7 due to signal loss in the emitter followers Q_5 and Q_6. The DC-gain is 50dB for 0% tuning and it varies by the same amount as ω_0 as expected from eq. 6. The phase characteristic in fig. 7 is obtained with $I_Q=52\mu A$ and is independent of tuning, because the dominant pole is independent of G_T, see eq. 5.

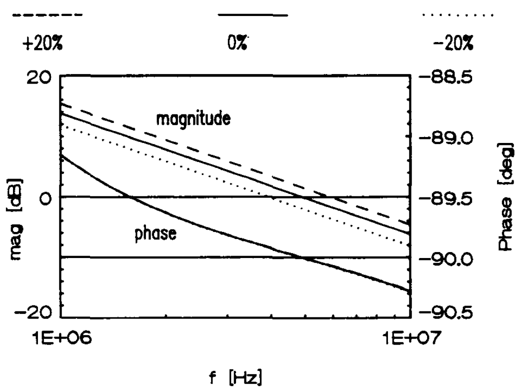

Fig. 7: Integrator simulations with different tuning.

Filter simulations

A fifth order elliptic lowpass filter with 5.0MHz cutoff frequency, 1.25dB passband ripple, 50.3dB stopband damping and transition width $\Omega_p/\Omega_s=1.39$ was designed and simulated using the circuits described.

The active-RC filter was implemented directly from the signal flow graph of the passive LCR prototype filter. All transconductors were chosen equal for optimum matching, with $R_1=6k\Omega$. First a nominal design was made, assuming the unity gain frequency of the integrators to be $\omega_0=1/R_1C_I$. Without tuning the cutoff frequency of this design was 12.6% below specification because of neglection of eq. 7 and signal loss in the emitter followers. All feedback capacitors can be scaled down by 12.6% to obtain the specified cutoff frequency and notch frequencies without frequency tuning. This scaled design can be implemented on chip, taking full advantage of the transconductor properties. In fig. 8 and 9 its response is compared with the ideal response. A Q-control current of 95μA is used to obtain the active filter response. There is additional insertion loss in the passband due to the low DC-gain of the integrators and some peaking near the passband edge. The latter is caused by poor output buffering by Q_5 and Q_6.

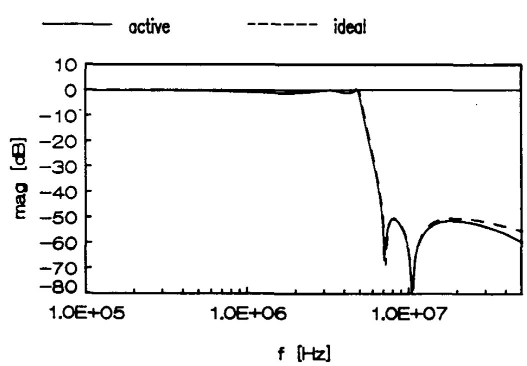

Fig. 8: Simulation of scaled design and ideal response.

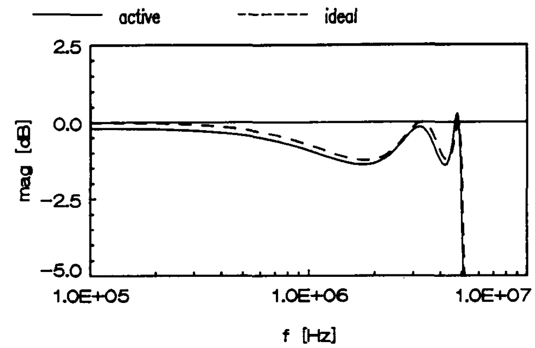

Fig. 9: Passband detail from fig. 8.

Conclusions

In this paper novel transconductor and integrator circuits are presented for bipolar integrated video frequency filters. The tunable transconductor principle is shown to result in good linearity up to $2V_{pp}$ input signal and good frequency response up to 70MHz. In the nominal case ($G_T=0$) the performance is even much better. The integrator circuit is based on a simple OTA with capacitive feedback. The right-half-plane zero caused by the finite transconductance of the OTA is moved to the left-half-plane by insertion of a variable resistance in the feedback path. Thus phase tuning is obtained besides frequency tuning. Simulations of a fifth order elliptic lowpass filter at 5.0MHz indicate that the circuits can be used for filter realization. Future research aims at improvement of the output buffers, the design of alternative transconductor circuits using the described principle, and on-chip tuning.

References

[1] S. Takagi *et. al.*,"A Differential Input/Output Integrator Without PNP Transistors and its Application to Leapfrog Filter Synthesis", Proc. ISCAS 1988, pp. 2855-2858.
[2] H. Hagiwara *et. al.*,"A Monolithic Video Frequency Filter Using NIC-Based Gyrators", IEEE J. Solid-State Circ., vol. 23, pp 175-182, Feb. 1988.
[3] F. Krummenacher and N. Joehl,"A 4-MHz CMOS Continuous-Time Filter with On-Chip Automatic Tuning", IEEE J. Solid-State Circ., vol. 23, pp 750-758, June 1988.
[4] C.S. Park and R. Schaumann,"Design of a 4-MHz Analog Integrated CMOS Transconductance-C Bandpass Filter" IEEE J. Solid-State Circ., vol. 23, pp 987-996, August 1988.
[5] K.W. Moulding *et. al.*,"Gyrator Video Filter IC with Automatic Tuning", IEEE J. Solid-State Circ., vol. SC-15, pp. 963-968, Dec. 1980.
[6] "BIMOS Design Manual", Internal publication of Philips Elcoma, Nijmegen, the Netherlands.
[7] "PHILPAC Processblock Manual", Internal publication of Philips Elcoma, Nijmegen, the Netherlands.
[8] C.F. Chiou and R. Schaumann, "Design and Performance of a Fully Integrated Bipolar 10.7 MHz Analog Bandpass Filter", IEEE J. Solid-State Circ., vol. SC-21, pp 6-14, Feb. 1986.